Journal of
Renewable Energy Research and Applications (RERA)

Vol. 5, No. 1, 2023, 11-19 *DOI: 10.22044/rera.2023.12674.1201*

Assessment of Solar Energy Availability and its Potential Applications in NEOM Region

Z. Aljohani[1], A. Asiri[1], S. Al-Awlaqi[2], T. Aljohani[2] and H. AbdelMeguid[1*]

1. Mechanical Engineering Department, Faculty of Engineering, University of Tabuk, Tabuk, Saudi Arabia.
2. Electrical Engineering Department, Faculty of Engineering, University of Tabuk, Tabuk, Saudi Arabia.

Received Date 03 February 2023; Revised Date 08 April 2023; Accepted Date 12 April 2023
**Corresponding author: habdelmeguid@ut.edu.sa (H. AbdelMeguid)*

Abstract
NEOM is a proposed megacity and business zone in the Kingdom of Saudi Arabia (KSA). It was announced in 2017 by Crown Prince Mohammed bin Salman with the goal of creating a hub for innovation and a hub for the future of living. NEOM is planned to cover an area of over 26,500 square miles, and will include a focus on sustainability and cutting-edge technology. The project is being backed by the Saudi Arabian government and private investment. The primary objective of KSA is to utilize the renewable energy resources in the NEOM region sustainably. This study evaluates the availability of solar energy in the NEOM region on a quantitative and qualitative basis, and a database of weather conditions such as temperature and wind speed is collected and processed. NEOM has favorable climate conditions with an average annual radiation incident energy of 12.54 GJ/m^2, wind speed of 15.68 km/h, and temperatures ranging from 16 to 38 $^\circ$C. Based on the analyzed data, the study investigates the potential of solar energy as a sustainable source and alternative to conventional fossil fuels. The utilization of solar energy could be applied in various ways including seawater humidification-dehumidification (HDH) desalination with productivity of 26-33 l/day/m^2, solar cooling with an average load of 15 MJ/day/m^2, green hydrogen production with rate of 41-47 mole/day/m^2, and electrical power generation with rate 4.2-6.8 MJ/day/m^2.

Keywords: *Solar energy; availability assessment, potential applications.*

1. Introduction

In October 2017, the Kingdom of Saudi Arabia introduced the NEOM project, which aims to construct a smart, environmentally friendly economic region with zero carbon emissions. The NEOM project covers a 465 km coastline along the Aqaba Gulf and coral reefs in the northwest of Saudi Arabia [1]. The project offers numerous benefits including economic opportunities and enhanced competitiveness among various economic sectors [2].

The development of new communities such as NEOM presents challenges, particularly in terms of a lack of natural resources such as water and clean energy. As a result, it is necessary to utilize the available renewable energy sources such as solar, wind, wave, and tidal energy to meet the demands of these communities [3–6]. Solar energy is a promising solution, as it is readily available in the Middle East and North Africa, particularly in the Arabian Peninsula, and can be utilized for a variety of applications including solar heating [7], solar cooling [8–10], desalination [11], green hydrogen production [12,13], and electrical energy generation [14, 15].

One potential application for the NEOM region is the desalination of seawater utilizing solar energy, which would provide a sustainable source of fresh water. Various solar-powered desalination technologies exist including thermal-driven membrane (TDM) [16–19], humidification-dehumidification [20–23], and solar stills (SS) [24–27]. TDM desalination offers benefits such as high system efficiency and water quality, intermittent operation, and low operating temperatures. SS desalination is simple and low-cost but has limited production capabilities. The performance of SS desalination can be improved through the use of various design features such as pyramidal or hemispherical shapes, internal or external condensers, solar reflectors with fins or wicks or phase-changing materials. HDH desalination offers high productivity but is complex in configuration and operation, and its

performance is dependent on the system configuration and energy source.

Another potential application is solar cooling, which can reduce the amount of traditional energy used in air conditioning systems for facilities and residential buildings. The solar cooling process utilizes solar power to drive a thermally-driven cooling process, reducing and controlling the temperature of water or air for conditioning. Several cooling cycle techniques exist including absorption cycles [8–10], desiccant cycles [28, 29], and solar mechanical cycles [30–32].

The NEOM green hydrogen project, the world's largest green hydrogen plant, utilizes renewable energy to produce green ammonia. Research is underway to increase the efficiency of converting solar energy into hydrogen using a combination of technologies [33–37]. The storage and transportation of hydrogen energy is facilitated through the use of ammonia, which serves as an enabler for the storage, transport, and use of renewable energy [38]. Ammonia can be burned with air to produce energy, serving as an alternative to solar and wind energy during periods of low supply power [39]. Efforts are currently underway to find the best methods for burning ammonia in thermal power plants [40]. Green ammonia is also being evaluated as a cost-effective option for decarbonizing maritime transport and as a fuel source for internal combustion engines [41].

Direct conversion of solar energy into a clean and sustainable source of electrical energy via solar photo-voltaic (PV) or flexible panels remains a crucial approach for supplying electricity to various sectors. Although PV conversion efficiency is low, ongoing research aims to optimize their application and increase their efficiency [42–45].

This research work assesses the availability of solar energy in the NEOM area based on data from the NASA project [46]. It also investigates the potential applications of solar energy including direct use for desalination or solar cooling and indirect use through conversion into green hydrogen or electric energy. The productivity of these applications is evaluated based on available data from literature for each month of the year.

2. Results and discussion

2.1. Assessment of solar energy

NASA POWER project [46] provided solar radiation and weather data for the NEOM region over the course of five years, from January 2017 to December 2021. Using this data, an arithmetic average was calculated for each day of each month to represent the daily average of solar radiation and weather conditions.

Figure 1 represents the various components of clear sky solar radiation for the NEOM region (located at 28˚05'43.8"N 35˚04'57.4"E) over the course of a year. The components included in the figure are global radiation, direct normal beam, diffuse sky radiation, and earth reflected radiation, along with ambient temperature and wind speed data for an average day of each month.

The data in figure 1 provides insight into the daily average of global solar radiation perpendicular to a surface, as well as the daily average of wind speed and temperature. The total solar radiation has an average value of 715 W/m^2 with a day length of approximately 12 hours during the winter, while it has an average value of 685 W/m^2 with a day length of more than 15 hours during the summer months. The total solar radiation is composed of the direct normal beam and sky diffuse radiation.

The direct normal beam has an average value of 600 W/m^2 during the winter months and decreases to 570 W/m^2 during the summer months, while the average sky diffuse radiation is 115 W/m^2. The earth reflected radiation has an average value of 85 W/m^2 in the winter months and increases to 115 W/m^2 during the summer months.

From processing the provided data from NASA POWER project [46], table 1 lists the total incident energy from solar radiation on a perpendicular surface for an average day of each month, as well as the annual total amount for the NEOM region. The data shows that the total annual incident energy of the global radiation, direct normal beam, and sky diffuse radiation are 12.54, 10.41, and 2.13 GJ/m^2, respectively, while the total incident energy of the earth reflected radiation is 1.82 GJ/m^2. The minimum values of the daily total incident energy of the global radiation and direct normal beam are 30.3 MJ/m^2 and 25.9 MJ/m^2 in December, while the maximum values are 38.4 MJ/m^2 and 32.1 MJ/m^2 in June, respectively.

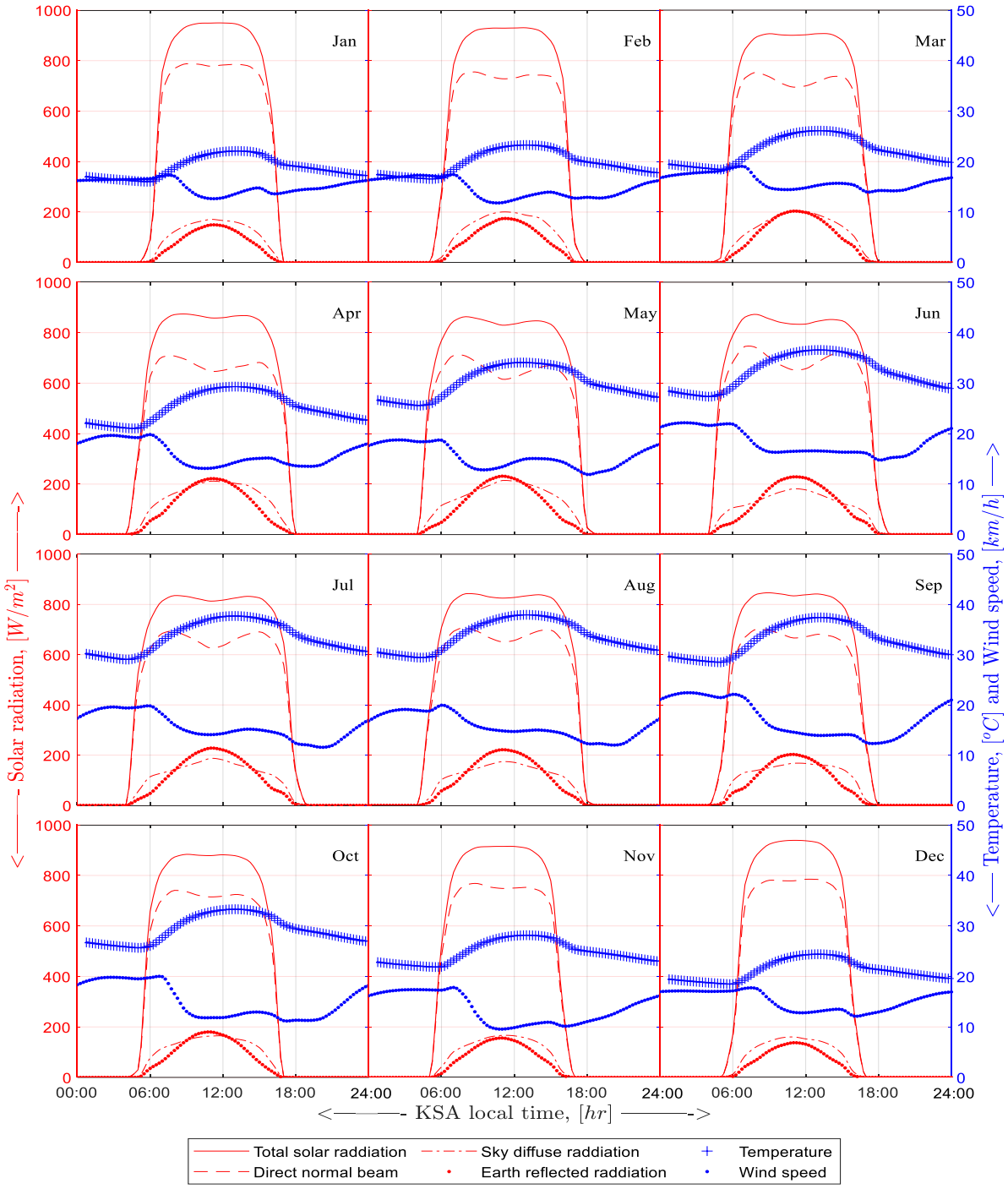

Figure 1. Clear sky conditions solar radiation and climate data for NEOM Region around the year for the average of each month processed and manipulated from NASA POWER project [46].

Table 1. Total incident energy from the solar radiation components of the average day of each month and year based on clear sky condition for NEOM region.

Solar radiation [MJ/m^2/day]	Jan	Feb	Mar	Apr	May	Jun	Jul	Aug	Sep	Oct	Nov	Dec	Total GJ/m^2/year
Total radiation	31.9	33.1	35.3	36.4	37.2	38.4	36.9	35.8	33.1	32.5	31.4	30.3	12.54
Direct normal beam	27.1	27.3	29.1	29.3	29.9	32.1	30.4	29.8	27.3	27.3	26.7	25.9	10.41
Sky diffuse radiation	4.8	5.8	6.2	7.1	7.3	6.3	6.5	6	5.8	5.2	4.7	4.4	2.13
Earth reflected radiation	3.4	4.2	5.2	5.9	6.2	6.3	6.3	6	5.2	4.4	3.6	3.1	1.82

2.2. Weather data

From processing the available data from NASA POWER project [46], table 2 records the minimum, average, and maximum temperature, and the average wind speed of the average day of each month through the year as well the annual average amount for the same weather aspects. The data depicts that, January has the minimum temperature trajectory around the year of minimum, average and maximum of about 16, 19, and 22 ˚C, respectively, while July and August have the maximum temperature trajectory of minimum, average and maximum of about 29, 33, and 38 ˚C, respectively. The wind speed has an average value over the year of 15.68 km/h.

Table 2. Minimum, average and maximum temperature, and average wind speed on the average day of each month for NEOM region.

		Jan	Feb	Mar	Apr	May	Jun	Jul	Aug	Sep	Oct	Nov	Dec	Avg.
Temperature [C]	Min	16.02	16.56	18.43	21.03	25.55	27.31	29.02	29.41	28.47	25.65	21.86	18.47	23.15
	Avg	18.80	19.68	22.10	25.11	29.86	32.04	33.35	33.56	32.69	29.22	24.74	21.14	26.86
	Max	22.11	23.29	26.13	29.31	34.08	36.57	37.70	37.94	37.41	33.32	28.17	24.41	30.87
Average wind speed [km/hr]		15.15	14.65	16.02	16.06	15.43	18.29	15.66	15.75	17.28	15.11	13.61	15.15	15.68

2.3. Potential application of solar desalination

Solar desalination

Due to the limited water resources and the availability of solar energy around the year, solar desalination is one of the most talented applications that can supply fresh water for the NEOM region. Solar desalination relies on several techniques including HDH, thermal membranes, and solar stills. The gain ratio of the HDH can be ranged from 0.81 to 4.23 [20–23], which depends on the design of the system and the use of multiple sources of energy. This method is considered one of the most productive methods, especially if it is combined with other thermal systems for heating water and air. The TDM method is characterized by medium productivity, which is obvious from the specific energy consumption (SEC) that ranges from 180 to 611 kWh/m^3 [16–19]. SS desalination is characterized by simple design and effortless operation that does not require trained workers or high maintenance costs, but SS is characterized by low production [24–27] compared to the other techniques. The performance of solar desalination technologies is listed in table 3.

Table 3. Performance of solar desalination technologies.

HDH Gain ratio		TDM, SEC, kWh/m^3		Solar still, Efficiency %	
Elzayed *et al*., 2021 [20]	0.99	Shafieian *et al*., 2020 [16]	611	Prakash and Jayaprakash, 2021 [24]	50.85
Mohamed *et al*., 2021 [21]	0.81	Criscuoli and Carnevale 2022 [17]	580	Abdullah *et al*., 2021 [25]	82.00
Abdel Dayem and AlZahrani, 2022 [22]	4.23	Zaragoza *et al*. 2014 [18]	400	Ahmed *et al*., 2021 [26]	50.55
Khalaf-Allah *et al*., 2022 [23]	1.45	Shafieian *et al*., 2020 [19]	180	Mohaisen *et al*., 2021 [27]	46.00

Figure 3 depicts the freshwater daily production of different solar powered desalination technologies around the year under NEOM region solar radiation and climate conditions. Figure 2 (a) illustrate the freshwater production from solar still methodologies. On the average basis, solar still produces 8 l/day/m^2 in the winter months and increases to 10 l/day/m^2 in the summer months. Figure 2 (b) shows the freshwater production from HDH techniques. On the average basis, HDH yields 26 l/day/m^2 in the winter months and grows to 33 l/day/m^2 in the summer months. Figure 2 (c) indicates the freshwater production from TDM systems. On the average basis, TDM returns 20 l/day/m^2 in the winter months and increases to 25 l/day/m^2 in the summer months. A comparison between the three technologies is presented in figure 2 (d), the figure illustrates that the HDH technologies have a large production compared to the other technologies. In this context, it should be noted that these technologies should be compared in terms of the cost of construction and periodic maintenance, as well as the extent of ease of operation and dependence on different types of energy, and the extent of their compatibility with the environment.

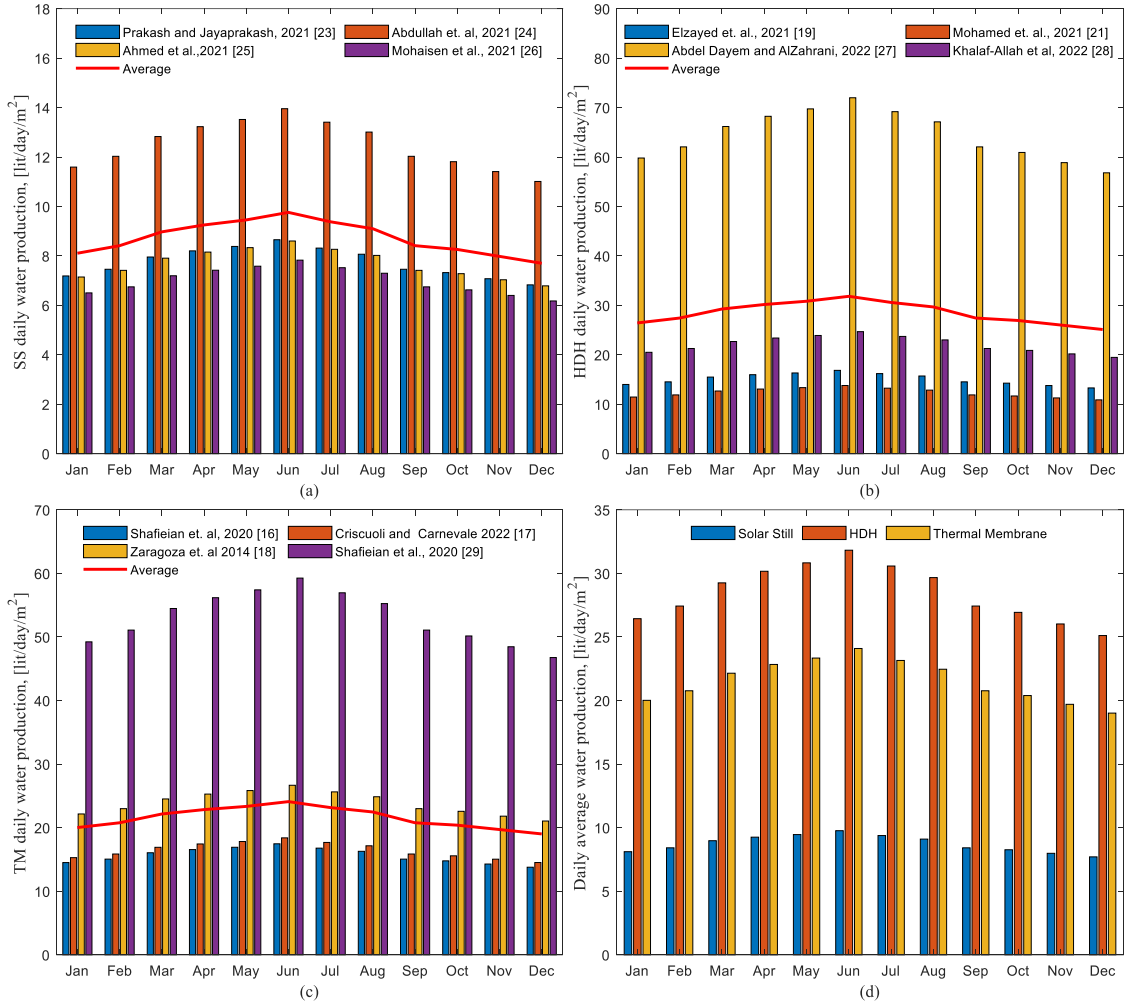

Figure 2. Daily freshwater production from solar desalination technologies based on NEOM region solar availability and climate conditions around the year.

Solar cooling

As shown in figure 1, the nature of the weather in NEOM region tends to be high temperatures that exceed 30 degrees Celsius from April to October. This makes the need for air conditioning in residential, administrative, and commercial buildings very necessary, so solar cooling is one of the important potential applications in NEOM area. Solar cooling technologies depend on the use of different pairs of moisture adsorption materials, which are designed and operated in different ways that affect their coefficient of performance, as listed in table 4.

Figure 3 illustrate the solar cooling load from different systems based on two-dimensional solar tracking water heaters. The solar cooling load varies from 10 to 20 MJ/day/m^2 with an average of 14 MJ/day/m^2 in the winter months and increases to 10 to 25 MJ/day/m^2 with an average of 17 MJ/day/m^2 in the summer months.

Table 4. Coefficient of performance of solar cooling technologies

Solar cooling, coefficient of performance	
El-Sharkawy *et al*., 2013-2014 [8–10]	0.53
Najeh *et al*., 2016 [47], Elsheniti *et al*., 2021 [48]	0.625
Liu *et al*., 2021 [49]	0.26
Chang *et al*., 2009 [50]	0.37

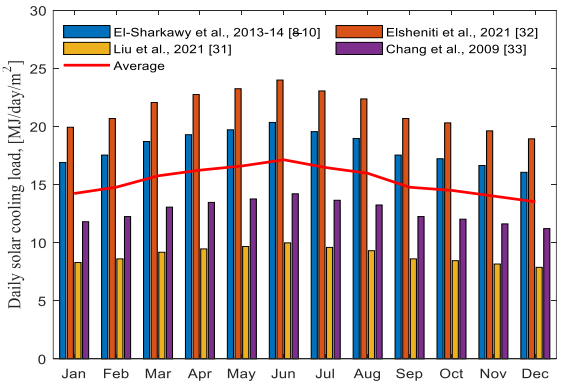

Figure 3. Daily solar cooling load based on NEOM region solar availability and climate conditions around the year.

Green hydrogen production

Green hydrogen can be produced at NEOM using photolysis, which is a process that uses light energy to split water into hydrogen and oxygen. In this process, sunlight is concentrated onto a photo-electrochemical cell, which uses the energy from the light to drive the electrolysis reaction. This allows for the production of hydrogen gas without the need for electrical power, which can be generated from renewable sources such as solar energy with solar to hydrogen efficiency (STH) ranged from 25% to 36%, as listed in TABLE 5. By using photolysis at NEOM, hydrogen can be produced in a clean and sustainable manner, helping to reduce greenhouse gas emissions and support the transition to a low-carbon energy economy.

Figure 4 represents the green hydrogen production at NEOM for each month of the year. The production of green hydrogen appears to be highest in the months of June, with a production rate of 47 mole/day/m^2, and lowest in the months of Jan and Dec, with a production rate of 38 mole/day/m^2. Overall, the production rate is relatively stable throughout the year, with small fluctuations around an average production rate of approximately 41 mole/day/m^2. This could indicate that the green hydrogen production at NEOM is relatively consistent and reliable but further analysis is needed to determine the causes of the fluctuations in production and the factors that influence the production rate.

Table 5. Green hydrogen production, STH efficiency.

Green Hydrogen production, STH efficiency	
Sun *et al*., 2022 [33]	25.00%
Nishiyama *et al*., 2021 [34] , Jieyang *et al*., 2016 [35]	30.00%
Wijayantha 2012 [36]	31.00%
Qiao *et al*., 2022 [37]	26.33

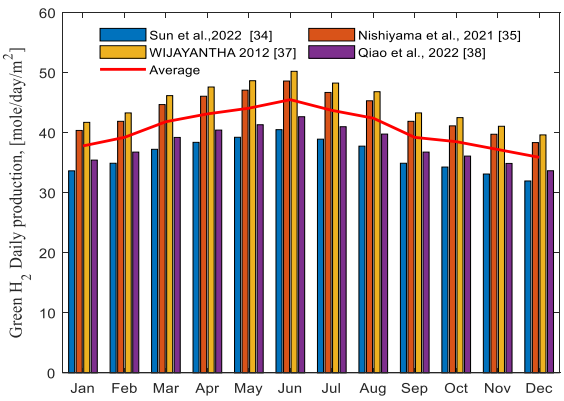

Figure 4. Daily green hydrogen production based on NEOM region solar availability and climate conditions around the year.

Electric generation

Electricity can be produced from photo-voltaic (PV) and thermos-photo-voltaic (TPV) systems at NEOM. Photo-voltaic (PV) systems convert sunlight into electrical energy using solar cells. Thermo-photo-voltaic (TPV) systems use heat from a fuel source or solar collectors to generate electricity by exciting a photovoltaic cell. Both methods produce electricity from renewable sources and support a low-carbon energy economy. By using both PV and TPV systems, NEOM can produce electricity from renewable sources in a clean and sustainable manner with conversion efficiency ranged from 12% to 18%, as listed in table 6, helping to reduce greenhouse gas emissions and support the transition to a low-carbon energy economy.

Table 6. PV and TPV conversion efficiency.

PV and TPV conversion efficiency	
Yildirim *et al*., 2022 [42]	17.79%
Arslan *et al*., 2020 [43]	13.56% - 13.89%
Sukumaran and Sudhakar, 2018 [44]	13.33 – 16.4%
Kumar *et al*., 2021 [45]	12-18%

Figure 5 represents the electricity production at NEOM using PV/TPV systems around the year. The production of electricity appears to be highest in the months of May and Jun, with a production range of 6.7 to 6.8 MJ/day/m^2, and lowest in the month of Nov, with a production range of 4.2 to 5.5 MJ/day/m^2. Overall, the production rate is relatively stable throughout the year, with small fluctuations around an average production rate of approximately 5.2 to 5.9 MJ/day/m^2. This could indicate that the electricity production at NEOM is relatively consistent and reliable but further analysis is needed to determine the causes of the fluctuations in production and the factors that influence the production rate.

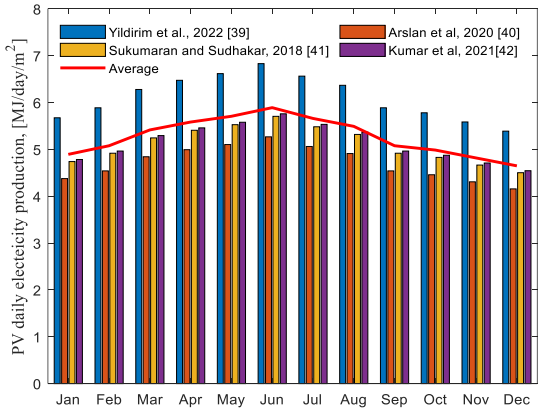

Figure 5. Daily PV electricity generation based on NEOM region solar availability and climate conditions around the year.

3. Conclusion

In conclusion, the study analyzed the solar energy potential of the NEOM region. The annual incident energy of the global radiation, direct normal beam, and sky diffuse radiation was found to be 12.54, 10.41, and 2.13 GJ/m^2, respectively. The weather data showed that the wind speed in the region had an average value of 15.68 km/h, and the temperature had minimum, average, and maximum values of 16, 19, and 22 ˚C in January, and 29, 33, and 38 ˚C in July and August, respectively.

- Solar Desalination: Solar desalination techniques including HDH, thermal membranes, and solar stills can provide fresh water for the NEOM region. HDH yields 26-33 l/day/m^2, thermal membranes yield 20-25 l/day/m^2, and solar stills yield 8-10 l/day/m^2. HDH is considered to be the most productive method compared to the other techniques.
- Average solar cooling load is 14 MJ/day/m^2 in winter and 17 MJ/day/m^2 in summer.
- Average green hydrogen production rate is 41 mole/day/m^2, with highest production rate in June (47 mole/day/m^2) and lowest in Jan/Dec (38 mole/day/m^2).
- Monthly electricity production rate is highest in May and June (6.7 to 6.8 MJ/day/m^2) and lowest in Nov (4.2 to 5.5 MJ/day/m^2) with an average of 5.2 to 5.9 MJ/day/m^2.

Further study is needed to determine the best technology that aligns with NEOM's goals of maximizing productivity while minimizing costs and environmental impact. The chosen technology should be cost-effective and minimize the negative impact on the environment. With the proper technology in place, NEOM can achieve its goal of producing renewable energy in a clean and sustainable manner, reducing greenhouse gas emissions, and supporting the transition to a low-carbon energy economy. By conducting this additional analysis, the team can ensure that the implementation of the technology is both efficient and sustainable, and that the goals of NEOM are met in a manner that benefits the environment and society.

4. Acknowledgment

The authors extend their appreciation to the Deanship of Scientific Research at the University of Tabuk for funding this work through Research no. S-1443-0026.

5. References

[1] NEOM : Made to chanage, 2022. (n.d.). https://www.neom.com/ (accessed December 7, 2022).

[2] NEOM - vision 2030, (2022). https://www.vision2030.gov.sa/v2030/v2030-projects/neom/ (accessed December 7, 2022).

[3] R. Farmani, D. Butler, D.V.L. Hunt, F.A. Memon, H. Abdelmeguid, S. Ward, C.D.F. Rogers, Scenario-based sustainable water management and urban regeneration, Proc. Inst. Civ. Eng. Eng. Sustain. 165 (2012) 89–98. https://doi.org/10.1680/ensu.2012.165.1.89.

[4] F.A. Memon, D. Butler, R. Farmani, H. Abdelmeguid, S. Atkinson, C. Rogers, D. Hunt, Urban Futures – Sustainability (Resilience) Evaluation of Water Infrastructure, 2011 AEESP Educ. Res. Conf. (2011).

[5] S. Ward, H. Abdelmeguid, R. Farmani, F.A. Memon, D. Butler, Sustainable water management - Modelling acceptability for decision support: A methodology, Urban Water Manag. Challenges Oppurtunities - 11th Int. Conf. Comput. Control Water Ind. CCWI 2011. 1 (2011).

[6] R. Farmani, D. Butler, F. Memon, H. Abdelmeguid, S. Ward, Sustainable water management for urban regeneration, Futur. Urban Water Solut. Livable Resilient Cities. (2011).

[7] M. Abu Mallouh, H. AbdelMeguid, M. Salah, A comprehensive comparison and control for different solar water heating system configurations, Eng. Sci. Technol. an Int. J. 35 (2022) 101210. https://doi.org/10.1016/j.jestch.2022.101210.

[8] I.I. El-Sharkawy, H. AbdelMeguid, B.B. Saha, Potential application of solar powered adsorption cooling systems in the Middle East, Appl. Energy. 126 (2014) 235–245. https://doi.org/10.1016/j.apenergy.2014.03.092.

[9] I.I. El-Sharkawy, H. Abdelmaguid, B.B. Saha, S. Koyama, T. Miyazaki, Performance Investigation of A Solar-Powered Adsorption Cooling System: A Case Study for Egypt, Int. Symp. Innov. Mater. Process. Energy Syst. 2013. (2013).

[10] I.I. El-Sharkawy, H. Abdelmeguid, B.B. Saha, Towards an optimal performance of adsorption chillers: Reallocation of adsorption/desorption cycle times, Int. J. Heat Mass Transf. 63 (2013) 171–182. https://doi.org/10.1016/j.ijheatmasstransfer.2013.03.076.

[11] M. Elsharkawy, H. AbdelMeguid, I.I. El-Sharkawy, L. Rabie, Experimental and theoretical investigation of decentralized desalination system, Mansoura Eng. J. 39 (2014).

[12] A. Nakamura, Y. Ota, K. Koike, Y. Hidaka, K. Nishioka, M. Sugiyama, K. Fujii, A 24.4% solar to hydrogen energy conversion efficiency by combining concentrator photovoltaic modules and electrochemical cells, Appl. Phys. Express. 8 (2015). https://doi.org/10.7567/APEX.8.107101.

[13] S. Sukpancharoen and N. Phetyim, Green hydrogen and electrical power production through the integration of CO2 capturing from biogas: Process optimization and dynamic control, Energy Reports. 7 (2021) 293–307. https://doi.org/10.1016/j.egyr.2021.06.048.

[14] H. Albalawi, M.E. El-Shimy, H. AbdelMeguid, A.M. Kassem, S.A. Zaid, Analysis of a Hybrid Wind/Photovoltaic Energy System Controlled by Brain Emotional Learning-Based Intelligent Controller, Sustainability. 14 (2022) 4775. https://doi.org/10.3390/su14084775.

[15] S.A. Zaid, H. Albalawi, H. AbdelMeguid, T.A. Alhmiedat, A. Bakeer, Performance Improvement of H8 Transformerless Grid-Tied Inverter Using Model Predictive Control Considering a Weak Grid, Processes. 10 (2022) 1243. https://doi.org/10.3390/pr10071243.

[16] A. Shafieian, M. Rizwan Azhar, M. Khiadani, T. Kanti Sen, Performance improvement of thermal-driven membrane-based solar desalination systems using nanofluid in the feed stream, Sustain. Energy Technol. Assessments. 39 (2020). https://doi.org/10.1016/j.seta.2020.100715.

[17] A. Criscuoli, M.C. Carnevale, Localized Heating to Improve the Thermal Efficiency of Membrane Distillation Systems, Energies. 15 (2022). https://doi.org/10.3390/en15165990.

[18] G. Zaragoza, A. Ruiz-Aguirre, E. Guillén-Burrieza, Efficiency in the use of solar thermal energy of small membrane desalination systems for decentralized water production, Appl. Energy. 130 (2014) 491–499. https://doi.org/10.1016/j.apenergy.2014.02.024.

[19] A. Shafieian, M. Rizwan Azhar, M. Khiadani, T. Kanti Sen, Performance improvement of thermal-driven membrane-based solar desalination systems using nanofluid in the feed stream, Sustain. Energy Technol. Assessments. 39 (2020). https://doi.org/10.1016/j.seta.2020.100715.

[20] M.S. Elzayed, M.A.M. Ahmed, M.A. Antar, M.H. Sharqawy, S.M. Zubair, The impact of thermodynamic balancing on the performance of a humidification dehumidification desalination system, Therm. Sci. Eng. Prog. 21 (2021). https://doi.org/10.1016/j.tsep.2020.100794.

[21] A.S.A. Mohamed, A.G. Shahdy, and M. Salem Ahmed, Investigation on solar humidification dehumidification water desalination system using a closed-air cycle, Appl. Therm. Eng. 188 (2021). https://doi.org/10.1016/j.applthermaleng.2021.116621.

[22] A.M. Abdel Dayem and A. AlZahrani, Psychometric study and performance investigation of an efficient evaporative solar HDH water desalination system, Sustain. Energy Technol. Assessments. 52 (2022) 102030. https://doi.org/10.1016/j.seta.2022.102030.

[23] R.A. Khalaf-Allah, G.B. Abdelaziz, M.G. Kandel, and A.S. Easa, Development of a centrifugal sprayer-based solar HDH desalination unit with a variety of sprinkler rotational speeds and droplet slot distributions, Renew. Energy. 190 (2022) 1041–1054. https://doi.org/10.1016/j.renene.2022.04.019.

[24] A. Prakash and R. Jayaprakash, Performance evaluation of stepped multiple basin pyramid solar still, Mater. Today Proc. 45 (2021) 1950–1956. https://doi.org/10.1016/j.matpr.2020.09.227.

[25] A.S. Abdullah, Z.M. Omara, F.A. Essa, A. Alarjani, I.B. Mansir, and M.I. Amro, Enhancing the solar still performance using reflectors and sliding-wick belt, Sol. Energy. 214 (2021) 268–279. https://doi.org/10.1016/j.solener.2020.11.016.

[26] M.M.Z. Ahmed, F. Alshammari, A.S. Abdullah, and M. Elashmawy, Experimental investigation of a low cost inclined wick solar still with forced continuous flow, Renew. Energy. 179 (2021) 319–326. https://doi.org/10.1016/j.renene.2021.07.059.

[27] H.S. Mohaisen, J.A. Esfahani, and M.B. Ayani, Improvement in the performance and cost of passive solar stills using a finned-wall/built-in condenser: An experimental study, Renew. Energy. 168 (2021) 170–180. https://doi.org/10.1016/j.renene.2020.12.056.

[28] A. Ramzy, H. AbdelMeguid, and W.M. ElAwady, A novel approach for enhancing the utilization of solid desiccants in packed bed via intercooling, Appl. Therm. Eng. 78 (2015) 82–89. https://doi.org/http://dx.doi.org/10.1016/j.applthermaleng.2014.12.035.

[29] A. Ramzy, W.M. Elawady, and H. Abdelmeguid, Modelling of heat and moisture transfer in desiccant packed bed utilizing spherical particles of clay impregnated with CaCl 2, Appl. Therm. Eng. 66 (2014) 499–506. https://doi.org/10.1016/j.applthermaleng.2014.02.031.

[30] R. Best and I. Pilatowsky, Solar assisted cooling with sorption systems: status of the research in Mexico and Latin America, Int. J. Refrig. 21 (1998) 100–115. https://doi.org/https://doi.org/10.1016/S0140-7007(97)00051-0.

[31] Y. Lu and J. Wang, Thermodynamics Performance Analysis of Solar-assisted Combined Cooling, Heating and Power System with Thermal Storage, Energy Procedia. 142 (2017) 3226–3233. https://doi.org/10.1016/j.egypro.2017.12.495.

[32] B.J. Huang, J.H. Wu, H.Y. Hsu, and J.H. Wang, Development of hybrid solar-assisted cooling/heating system, Energy Convers. Manag. 51 (2010) 1643–1650. https://doi.org/https://doi.org/10.1016/j.enconman.2009.07.026.

[33] R. Sun, C.L. Yang, M.S. Wang, and X.G. Ma, High solar-to-hydrogen efficiency photocatalytic hydrogen evolution reaction with the HfSe2/InSe heterostructure, J. Power Sources. 547 (2022) 232008. https://doi.org/10.1016/j.jpowsour.2022.232008.

[34] H. Nishiyama, T. Yamada, M. Nakabayashi, Y. Maehara, M. Yamaguchi, Y. Kuromiya, Y. Nagatsuma, H. Tokudome, S. Akiyama, T. Watanabe, R. Narushima, S. Okunaka, N. Shibata, T. Takata, T. Hisatomi, and K. Domen, Photocatalytic solar hydrogen production from water on a 100-m^2 scale, Nature. 598 (2021) 304–307. https://doi.org/10.1038/s41586-021-03907-3.

[35] J. Jia, L.C. Seitz, J.D. Benck, Y. Huo, Y. Chen, J.W.D. Ng, T. Bilir, J.S. Harris, and T.F. Jaramillo, Solar water splitting by photovoltaic-electrolysis with a solar-to-hydrogen efficiency over 30%, Nat. Commun. 7 (2016). https://doi.org/10.1038/ncomms13237.

[36] K.G.U. Wijayatha, Photoelectrochemical cells for hydrogen generation, 2012. https://doi.org/10.1533/9780857096371.1.91.

[37] H. Qiao, Y. Zhang, Z.H. Yan, L. Duan, L. Ni, J. Bin Fan, A type-II GaN/InS van der Waals heterostructure with high solar-to-hydrogen efficiency of photocatalyst for water splitting, Appl. Surf. Sci. 604 (2022) 154602. https://doi.org/10.1016/j.apsusc.2022.154602.

[38] M.J. Palys and P. Daoutidis, Using hydrogen and ammonia for renewable energy storage: A geographically comprehensive techno-economic study, Comput. Chem. Eng. 136 (2020) 106785. https://doi.org/10.1016/j.compchemeng.2020.106785.

[39] D. Pashchenko, R. Mustafin, and I. Karpilov, Ammonia-fired chemically recuperated gas turbine: Thermodynamic analysis of cycle and recuperation system, Energy. 252 (2022). https://doi.org/10.1016/j.energy.2022.124081.

[40] X. Chen, Q. Liu, W. Zhao, R. Li, Q. Zhang, and Z. Mou, Experimental and chemical kinetic study on the flame propagation characteristics of ammonia/hydrogen/air mixtures, Fuel. 334 (2023) 126509. https://doi.org/10.1016/j.fuel.2022.126509.

[41] binbin wang, C. Yang, H. Wang, D. Hu, B. Duan, yinyan Wang, Study on Injection Strategy of Ammonia/Hydrogen Dual Fuel Engine Under Different Compression Ratios, SSRN Electron. J. 334 (2022) 126666. https://doi.org/10.2139/ssrn.4190900.

[42] M.A. Yildirim, A. Cebula, and M. Sułowicz, A cooling design for photovoltaic panels – Water-based PV/T system, Energy. 256 (2022). https://doi.org/10.1016/j.energy.2022.124654.

[43] E. Arslan, M. Aktaş, and Ö.F. Can, Experimental and numerical investigation of a novel photovoltaic thermal (PV/T) collector with the energy and exergy analysis, J. Clean. Prod. 276 (2020). https://doi.org/10.1016/j.jclepro.2020.123255.

[44] S. Sukumaran and K. Sudhakar, Performance analysis of solar powered airport based on energy and exergy analysis, Energy. 149 (2018) 1000–1009. https://doi.org/10.1016/j.energy.2018.02.095.

[45] A. Kumar Behura, A. Kumar, D. Kumar Rajak, C.I. Pruncu, and L. Lamberti, Towards better performances for a novel rooftop solar PV system, Sol. Energy. 216 (2021) 518–529. https://doi.org/10.1016/j.solener.2021.01.045.

[46] NASA POWER project, (2021). https://power.larc.nasa.gov/ (accessed October 31, 2021).

[47] G. Najeh, G. Slimane, M. Souad, B. Riad, E.G. Mohammed, Performance of silica gel-water solar adsorption cooling system, Case Stud. Therm. Eng. 8 (2016) 337–345. https://doi.org/10.1016/j.csite.2016.07.002.

[48] M.B. Elsheniti, A. Rezk, M. Shaaban, M. Roshdy, Y.M. Nagib, O.A. Elsamni, and B.B. Saha, Performance of a solar adsorption cooling and desalination system using aluminum fumarate and silica gel, Appl. Therm. Eng. 194 (2021). https://doi.org/10.1016/j.applthermaleng.2021.117116.

[49] Y.M. Liu, Z.X. Yuan, X. Wen, C.X. Du, Evaluation on performance of solar adsorption cooling of silica gel and SAPO-34 zeolite, Appl. Therm. Eng. 182 (2021). https://doi.org/10.1016/j.applthermaleng.2020.116019.

[50] W.S. Chang, C.C. Wang, and C.C. Shieh, Design and performance of a solar-powered heating and cooling system using silica gel/water adsorption chiller, Appl. Therm. Eng. 29 (2009) 2100–2105. https://doi.org/10.1016/j.applthermaleng.2008.10.021.